University of Nevada, Reno

SNOWPACK CONTROLS ON HYDROLOGIC RESPONSE TO EXTREME RAIN-ON-SNOW EVENTS IN THE NORTHERN SIERRA NEVADA

A Thesis Submitted in Partial Fulfillment of the Requirements for the Degree of Master of Science in Hydrology

by Lisa J. Katz

Dr. Adrian A. Harpold, Thesis Advisor

August 2021

THE GRADUATE SCHOOL

We recommend that the thesis
prepared under our supervision by

LISA J. KATZ

entitled

SNOWPACK CONTROLS ON HYDROLOGIC RESPONSE TO EXTREME RAIN-ON-SNOW EVENTS IN THE NORTHERN SIERRA NEVADA

be accepted in partial fulfillment of the
requirements for the degree of

MASTER OF SCIENCE

Adrian A. Harpold, Ph.D.
Advisor

Stephen Drake, Ph.D.
Committee Member

Erin Hanan, Ph.D.
Committee Member

Benjamin Hatchett, Ph.D
Graduate School Representative

David W. Zeh, Ph.D., Dean
Graduate School

August, 2021

Abstract

Continuous, near-real time predictions of winter flooding are critical to balancing the protection of life and property with providing water resources for consumptive use in California's northern Sierra Nevada. Rain-on-snow (ROS) events are a major cause of floods in the region and are expected to increase as a result of climate change. During ROS, the amount of terrestrial water input (TWI) draining from the snowpack is the major driver of floods and depends on the snowpack's capacity to refreeze liquid water, its transmissivity, and the magnitude of snow melt during the event. The outcome is an interplay between (1) the amount and intensity of precipitation, (2) the antecedent conditions of the snowpack and (3) the potential for incoming energy to melt snow and drain additional water. An incomplete understanding and insufficient measurement of these interacting processes limits the skill of flood prediction in mountain regions. In this study, antecedent snowpack conditions, specifically cold content, density, liquid water content and SWE, are examined to understand how these factors modulate TWI during ROS. Data from three SNOTEL stations, common in the Western U.S., across a 500-m elevation gradient on the eastern side of California's Sierra Nevada mountains are used as input to a physically-based model that simulates liquid water drainage explicitly (SNOWPACK). Hourly forcing parameters were developed to calibrate and validate the SNOWPACK model to the

SNOTEL stations spanning water years 1981-2019 and 149 ROS events. During the 149 historical events, the snowpack mitigated TWI for 80% of events, 13% had no mitigation, and 7% had conditions for active melt. Mean TWI increased 32% from the lowest elevation (58 *mm* of water) to the highest elevation (85 *mm* of water). As expected, the amount of TWI depends on total rainfall, however, that events with TWI/rain ratios > 1.0 produce the largest event streamflows. When antecedent conditions were varied in reasonable ways, total TWI response varies 46% on average across eight extreme events. A key result is that snowpack cold content explains the majority of TWI variability. Riper snowpacks generated the highest TWI values for most events, with a 1 MJ decrease in cold content corresponding to 0.74 more TWI. Our results highlight the importance of cold content in TWI response across realistic antecedent conditions. Cold content is rarely measured and effectively not included in operational flood forecast models. As ROS becomes increasingly frequent in a warming climate, enhanced observations of cold content and modeling could have important implications for improved flood forecasting.

Acknowledgements

Foremost, I'd like to thank Dr. Adrian Harpold, my master's thesis advisor, for working with me to develop research questions, ideas, processes, interpretations and with the writing. Dr. Harpold has guided me through the each step of the scientific process and introduced me opportunities that were the highlight of my graduate school experience. Thank you for funding this research and always providing me with the tools I needed to be successful.

Drs. Anne Nolin and Alexandra Lutz for the seemless operation, top-notch excellence of the Graduate Program in Hydrological Sciences at University of Nevada, Reno (UNR), and for always helping me out when in a bind. Dr. Nolin additionally for providing opportunities to enhance my graduate school experience, such as the NASA SnowEx program and UNR's WaterWorks.

Dr. Michael Dettinger and CW3e for funding this research, significant contributions to the research focus and review of our results. The Nevada NASA Space Grant Consortium and Nevada EPSCOR for providing funding for this work as well as opportunities to present our research at EPSCOR conferences. Additionally, thank you to Karin Peternel, Tina Triplett and the Nevada Water Resources Association for scholarship funding and guidance.

I'd like to thank my mother, Leslie Riddel, and my father, David Katz, for always putting up with my antics, for their love and support no matter what I do. Thank you to Dr. Erica Bigio for employing me as a TA during graduate school, and for her support. Drs. Stephen Drake, Erin Hanan and Benjamin Hatchett for their service as my master's thesis committee members, as collaborators and for their genius in improving our research. Dr. Keith Jennings teaching me how to dig my first snowpit, for introducing me to the SNOWPACK model and installing it on my computer.

A HUGE thank you to Dr. Sebastian Krough who also installed SNOWPACK on my computer when I couldn't figure out how to incorporate and compile SNOWPACK with the Richards Equation, without his help this research would not have been possible. Additionally, Drs. Krough and Gabe Lewis have guided and improved this research, and me personally, correcting countless mistakes I've made and teaching me ways to enhance my scientific skills. Dr. Hamideh Safa for her support and Python assistance. Dr. Seshadri Rajagopal for his early contributions to the research focus.

I'd like to thank my colleagues at Nevada Mountain Ecohydrology Lab, especially Ava Cooper for helping me start with Python, Gary Sterle for being a supportive and helpful office-mate and collaborator, Lauren Bolotin for downloading data and overall support, Josh Sturtevant for his assistance with fieldwork and Python support, and Anne Heggli for her research ideas

and conceptual understanding.

Last but not least, I'd like to give a sincere thank you to Jeff Anderson with the Natural Resources Conservation Service, Nevada Snow Survey, for taking me in as a wonky Earth Team Volunteer, showing me how to use a federal sampler, edit data, and encouraging me to apply for the Pathways internship with the Colorado Snow Survey. You got me started, thank you Jeff!

Contents

List of Tables

List of Figures

Key Points:

1. A calibrated and validated physical snow model reproduces SWE responses and predicts TWI during extreme rain on snow (ROS) events.
2. TWI varies 26-68% during eight large ROS events using variable mid-winter antecedent snowpack conditions.
3. Antecedent cold content explains TWI variability, with very wet events and low cold content snowpacks leading to the largest TWI response.

1 Introduction

Rain-on-snow (ROS) events cause the largest stream and river floods in many parts of the world, with both the storm characteristics and snowpack conditions sensitive to climate change effects (Kattelmann, 1996; Kroczynski, 2004; Marks, Kimball, et al., 1998; Ohba & Kawase, 2020; Rössler et al., 2013; Sui & Koehler, 2001). ROS events are any storm that causes significant rain onto an existing snowpack, with the largest effects typically in maritime regions with large potential for winter rain events (Musselman, Lehner, et al., 2018). In the Sierra Nevada mountains, USA, ROS is often associated with atmospheric river events that produce large rainfall amounts and a warm, humid atmosphere that can melt the snowpack (*Glossary of Meteorology: Atmospheric River* 2018; Guan et al., 2016; Kim et al., 2013; Henn et al., 2020). Consequently, the existing snowpack and its response

during ROS events (i.e. melting or not) can be critical for determining flood potential (Würzer et al., 2016; Garvelmann, Pohl, & Weiler, 2015). The future effects of ROS events are complicated by a rising snow-line and less area for ROS response (Klos, Link, & Abatzoglou, 2014), more extreme precipitation (Santer et al., 2007), a greater proportion of rain (less snow) falling on existing snowpacks (Knowles, M. D. Dettinger, & Cayan, 2006), and high intensity precipitation (Trenberth, 2011). Although the snow line is rising in many areas (Knowles, M. D. Dettinger, & Cayan, 2006), like the Sierra Nevada mountains (Hatchett et al., 2017), climate models suggest that mid elevations (1,500-2,500 $m.a.s.l$) will have an increase in ROS frequency, with more water available for runoff and 20-200% greater flood risk (Musselman, Lehner, et al., 2018). Less snow water equivalent and lower cold content at all elevations will make the melt response more sensitive to larger energy inputs (Luce & Tarboton, 2009), causing earlier and more intermittent snowmelt (Musselman, Clark, et al., 2017). However, future ROS response is difficult to predict because it depends on antecedent snowpack conditions (i.e. SWE, cold content, density, etc.) and its interactions with specific storm characteristics (i.e. rainfall amount and intensity, wind speed, temperature and humidity, etc.).

Terrestrial water input (TWI) is the amount of liquid water from the atmosphere that reaches the soil surface. When a snowpack is present, liquid

water that drains through the snowpack becomes TWI. TWI can be composed of rainfall, snowmelt, and/or liquid water stored the snowpack. These inputs, in addition to other antecedent conditions like soil moisture and reservoir levels, are key determinants of hydrological flood risk. TWI is affected by the amount and intensity of rainfall, refreezing of rainfall within the snowpack, and the potential for incoming energy to melt snow and drain additional water. Previous studies have shown that similar amounts of rainfall events can produce very different amounts of TWI due to drainage of liquid water and melt processes (Kroczynski, 2004). For wet snowpacks, the amount of initial snowpack water that drains to TWI depends primarily on rainfall amount. If the water is draining via simpler matrix flow, rainfall percolates through the pore spaces between snow grains from the top-down, filling up any undersaturated areas and eventually forcing out initial snowpack water once the snowpack's maximum water holding capacity is reached (Singh et al., 1998). Sub-zero temperature snowpacks (i.e. cold content < 0) will freeze rain on top of or within the snowpack, which can create a layer of ice with higher density and release latent and sensible heat that warms the snowpack. In many conditions, rain will enhance preferential flow, isolated areas of higher conductivity and liquid water content that tend to increase drainage relative to matrix flow (Waldner et al., 2004; Dozier et al., 1989; Schneebeli, 1995). Warm, moist air masses can transfer

latent and sensible heat into the snowpack and are thought to be the primary energy input for melt during ROS (Marks, Kimball, et al., 1998; Würzer et al., 2016), as well as longwave radiation from a cloudy atmosphere (Würzer et al., 2016; Mazurkiewicz, Callery, & McDonnell, 2008). Periods of high winds increase turbulent transfer of heat, promoting snow melt that augments rainfall and increases TWI (Marks, Kimball, et al., 1998; Kroczynski, 2004). Evidence is emerging that TWI variability during ROS events is mediated by antecedent snowpack conditions in ways that can switch the system from completely storing incoming rainfall to draining rainfall and stored snowpack water (Garvelmann, Pohl, & Weiler, 2015). The controls of antecedent snowpack conditions on ROS flood risk are not well understood and are a poorly constrained source of error for current and future operational streamflow forecasting models.

Meltwater freezing, snow melt and drainage are very difficult processes to simulate even with the most advanced physically based, energy balance model. In the most advanced physically representative snowpack modes, like SNOWPACK (Bartelt & Lehning, 2002; Lehning, Bartelt, Brown, & Fierz, 2002; Lehning, Bartelt, Brown, Fierz, & Satyawali, 2002), ice and liquid water water content are tracked in finite snow layers using mass and energy conserving equations. Energy inputs to the snowpack need to be fully resolved (i.e. longwave and shortwave radiation) in order to capture

the melt dynamics caused by turbulent and radiative energy and typically requires calibration of variables like surface roughness. In general, 'excess' energy above $0°C$ melts the ice matrix and any energy below $0°C$ freezes meltwater in ways that are mediated by the hydraulic conductivity and water content using the Richards equation (Richards, 1931; Wever, C. Fierz, et al., 2014). While SNOWPACK's finite element grid is a large improvement over most multi-layer snow models, it still does not capture preferential flow that tends to increase TWI above matrix flow estimates (Wever, Würzer, et al., 2016) nor the role of hillslope processes that can transmit water laterally before reaching the soil surface (Bartelt & Lehning, 2002). Its worth noting that model calibration and validation of ROS-mediated processes is challenged by a dearth of direct measurements, with key variables like cold and liquid water content only made in very limited conditions, and variables like SWE and snow density at resolutions that are often insufficient for hourly (or finer) physical models. In contrast to sophisticated snowpack models, most operational snowmelt models, like SNOW-17 (E. Anderson, 2006) use temperature index approaches that only require temperature and precipitation as input variables. SNOW-17 still retains some foundations of an energy balance by estimating energy inputs and tracking snowpack cold and liquid water content based on empirical relationships from a single site, but is a bulk model with calibrated, empirical parameters. E. Anderson (2006)

recognized that periods with warm temperatures, high humidity, and strong winds, characteristic of large ROS events, where SNOW-17 under-predicts melt. Despite a multitude of new field and remote observations, few measurements of snowpack conditions can be used by operational forecasters to tune or validate their models. This has left the operational community in the maritime western U.S. focused on improvements to ensemble hydrometeorological forecasts that use simpler, deterministic hydrology models. Given recent extreme ROS events and projections for increased ROS flooding in the Sierra Nevada (Musselman, Lehner, et al., 2018), a better understanding of the role of snowpack antecedent conditions on TWI response and its importance for operational forecasting is needed.

Water management in the northern Sierra Nevada mountains of California and Nevada, and other maritime mountains globally, is challenged by ROS. ROS events in winter produce floods, while at the same time reservoirs need to be filled by snowmelt to prepare for seasonal summer droughts. This leads to the inevitable 'water managers dilemma' that requires water supply for late summer demand, while maintaining empty storage capacity to accommodate winter storm runoff and protect growing urban areas from flooding (Brekke et al., 2014). The highly variable climate of the region (Dettinger et al., 2004) leads to 'weather whiplash', where rapid transitions between dry and wet conditions further stress water management institu-

tions and are expected to increase in this area (Swain et al., 2018). An important recent example from the northern Sierra Nevada is the the recent 2012–2016 drought followed by the winter 2017 flooding and Oroville Dam spillway incident. The potential to increase lead times during ROS events to better manage reservoirs, termed 'forecast informed reservoir management', could have potentially mitigated some of the risk for snowpack melt and under-predicted reservoir inflows (Brekke et al., 2014; White et al., 2019; Delaney et al., 2020). Henn et al. (2020) estimated that ~40% of the Oroville flood inflows came from snowmelt that was concentrated at low to medium elevations (Henn et al., 2020). Work in Switzerland (Würzer et al., 2016) suggests that high elevation snowpack can store rainfall during these large events. SWE observations in the Sierra Nevada from Henn et al. (2020) support these findings, however the impact of high-elevation storage for catchment-scale TWI inputs and streamflow forecasting are not well quantified. In this study, we focus on a transect of snow and hydrometeorological measurements in the Sagehen Creek watershed in the northern Sierra Nevada to calibrate and validate the SNOWPACK model. We use the validated model in a historical (hindcasting) approach and a scenario analysis to determine the role of antecedent snowpack conditions on hydrological response to historical ROS events and a scenario analysis of antecedent conditions. Our work is motivated by the following research questions:

1. How does terrestrial water input (TWI) vary during events with different rainfall amounts?
2. How does TWI vary during events with different antecedent snowpack conditions?
3. Which antecedent conditions are most predictive of TWI during extreme events?

We expect that our results can help inform the value of the current monitoring network that focuses on SWE and snow depth, and determine which snowpack conditions should be a focus for validating models and improving forecast information.

2 Methods

2.1 Study sites

Study sites were located on the leeward side of California's northern Sierra Nevada crest, north of Interstate 80 and the Town of Truckee, and west of California Highway 89. The Sierra Nevada features a maritime climate with cool, wet winters. Snow storms arrive as early as November, the snowpack begins to accumulate in January and is typically ablated by June. Winters are characterized by deep snowpacks with less cold content compared to similar continental sites (Jennings, Kittel, & Molotch, 2018).

Figure 2.1 shows snow modeling locations at three sites within the Natural Resources Conservation Service (NRCS) SNOTEL network, SNOTEL 541 Independence Lake (S-2541, 39°49' N, 120°28'23"), SNOTEL 539 Independence Camp (S-2124, 39°42'75" N, 120°31'34"), and SNOTEL 540 Independence Creek (S-1962, 39°42'75" N, 120°31'34"). The naming convention we use for these sites is S-, followed by the elevation of the site in meters. S-2124 sits on the shore of Independence Lake (2.83 km^2 surface area). All three study sites are characterized by flat surfaces in small forest gaps. The dominate tree species are Jeffery Pine (*Pinus jeffreyi*) and Ponderosa Pine (*Pinus ponderosa*).

Table 2.1 provides a summary of environmental variables at the study sites. Mean canopy height is one meter higher at S-2541 than S-2124, and almost 5 meters higher than S-1962. Canopy coverage and leaf area index (LAI) at S-2541 and S-2124 is more than double that at S-1962. The average windspeed at S-2541 is one meter per second higher than that at S-2124 and S-1962. S-2541 has greater than twice the average peak SWE of S-2124 and three times the average peak SWE of S-1962.

2.2 Snow model

The SNOWPACK snow model was used for this study. SNOWPACK is a one-dimensional, multi-layer, physically-based model developed by the

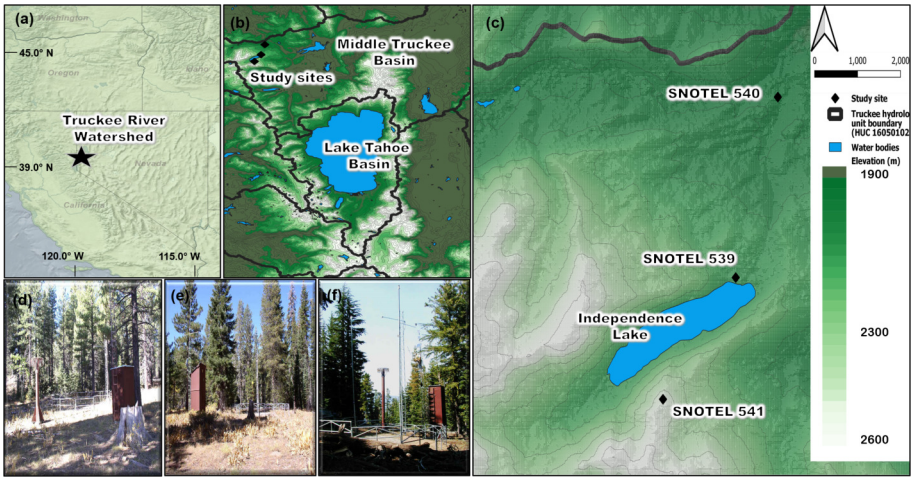

Figure 2.1. Study sites. The location of the Truckee River Watershed, on the border California and Nevada, within the western United States (a). A topographical map showing two basins within the Truckee River Watershed, the Middle Truckee Basin and the Lake Tahoe Basin. The study sites are located in the northwest corner of the Middle Truckee Basin. (b). A topographical map of the three study sites and their proximity to Independence Lake. The thin, solid lines are 100m contours (c). Photos of SNOTEL weather stations at the study sites, SNOTEL 540 Independence Creek (S-1962, d), SNOTEL 539 Independence Camp (S-2124, e), and SNOTEL 541 Independence Lake (S-2541, f).

Swiss Federal Institute for Snow and Avalanche Research. SNOWPACK was originally intended for daily operational avalanche risk assessment, however its usefulness is unmatched for ROS research because unlike other snow models, SNOWPACK implements the full Richards equation (RE) to provide a more accurate description of water flow through the snowpack.

Table 2.1. Study sites summary.

Site	Elevation (m)	Peak SWE (mm) [1]	Mean canopy height (m)[2]	Canopy cover $(\%)$[2]	LAI[2]	Average windspeed (m/s)[1]
S-2541	2541	1157	9.9	44.6	1.7	3.6
S-2124	2124	487	8.5	54.8	2.2	2.5
S-1962	1962	378	5.1	21.1	0.8	2.2

[1] Averages over water years (WYs) 1981-2019.
[2] Calculated within a 20 m radius from the center of the SNOTEL.

The RE outputs better agree with the timing and quantity of observed snowpack runoff at daily and seasonal timesteps, particularly in stratified snowpacks common to the northern Sierra Nevada. The RE calculates differences in capillary suction between layers (Wever, C. Fierz, et al., 2014). SNOWPACK with full implementation of the RE was chosen for this study to accurately represent liquid water dynamics in a variety of conditions.

SNOWPACK is documented in Bartelt & Lehning (2002), and Lehning, Bartelt, Brown, & Fierz (2002) and Lehning, Bartelt, Brown, Fierz, & Satyawali (2002). Model inputs can vary, however, we used the following commonly found datasets: air temperature, precipitation, relative humidity, ground surface temperature, windspeed, incoming shortwave and longwave radiation. The model incorporates the three phases of water (ice, water, and water vapor) into the simulated snowpack. Snowpack state is based on the principles of conservation of mass, energy and momentum by implicitly and sequentially solving a set of four governing differential equations for bulk temperature, vapor diffusion, water transport, and settlement. SNOWPACK incorporates the underlying assumptions that creep movements and water flow equal zero, all lateral temperature and vapor pressure gradients equal zero, and at any given time all constituents are at the same bulk temperature.

Unique snowpack layers are discretized by SNOWPACK into a finite element grid, based on the Lagrangian Gauss-Siedel finite element method.

The four governing differential equations are solved for each element in the grid independently. Finite elements can be added to or subtracted from an existing grid to accommodate changes in snow depth. Phase change processes occur at the surface and subsurface of the element. Meltwater refreezing, for example, is a volumetric heat source that happens when the bulk temperature of the element is below $0°C$ and meltwater is present (meltwater is always assumed to be at $0°C$). Refreezing meltwater increases volumetric ice content and decreases volumetric water content of the element.

The SNOWPACK model is well regarded for its treatment of snowpack microstructure. The model uses four independent microstructure parameters: sphericity, dendricity, grain size and bond size, with additional derivations of the primary parameters, such as coordination number. Changes in sphericity and dendricity happen much faster in wet snow than in dry snow and are treated separately within the model. Wet snow metamorphism in SNOWPACK is based on an empirical relationship for the volume growth of grains as a function of the mass fraction of liquid water. SNOWPACK assumes that wet snow bond growth is dominated by pressure sintering[1] because there is a lack of data and theory on wet snow bond growth. This treatment is considered simplistic, but advanced compared to the treatment

[1] Density increases from ice-grains moving closer together under the self-weight of the snowpack.

used in other models.

2.3 Snow model configuration

SNOWPACK was initialized with two soil layers and no snow layers, and run consecutively for 40 water years (WYs) 1981 to 2019. The model was run at a 15 minute integration step length, which was consistent with implementation of the Richards Equation, and results were output hourly. The RE was used for both water and soil transport schemes:

$$RE = \frac{\partial \theta}{\partial t} = \frac{\partial}{\partial z}[K(\theta)(\frac{\partial h}{\partial z} + 1)] \tag{2.1}$$

Where K is hydraulic conductivity,

h is the matric head induced by capillary action,

z is the elevation above a vertical datum,

θ is the volumetric water content,

t is time.

In common practice, observed snow depth is used as a forcing dataset in SNOWPACK and the setting 'enforce measured snow heights' is turned on.[2] In this configuration, the model uses measured snow depth as a proxy for

[2] standard, Intercantonal measurement and Information System (ImIS). ImIS is a network of snowpack monitoring stations in Switzerland, where the SNOWPACK model was developed and is used operationally in avalanche risk assessment.

precipitation inputs to force the mass balance. For the scenario analysis, however, the design required that precipitation inputs were independent of modeled snow depth. Therefore snow depth is omitted from model forcings and the aforementioned setting is turned off.

Realistic estimates of snowpack TWI require that models accurately represent snowpack-forest interactions (Gouttevin et al., 2015). Forest clearings accumulate, redistribute and melt snow differently than adjacent forested areas (Golding & Swanson, 1986) or areas in the open (Marks & Winstral, 2001). The tree canopy affects snowpack mass and energy budgets in many ways, such as intercepting falling snow, filtering shortwave radiation and buffering wind. Snowpacks <15 m from tree canopies show greater snow variability than areas >15 m from tree canopies (Broxton et al., 2015).

To tune the model, we characterized the forest surrounding each study site using LIDAR scans. Average canopy heights and percent canopy coverage were calculated for radii 10, 20, and 30 m from the study site center. LAI was estimated using a maximum value of $4m^2/m^2$ from the west shore of Lake Tahoe, CA, and multiplied by the percentage canopy cover. Simulations for ten water years were evaluated against observations of SWE with measured values for canopy height, canopy throughfall, and LAI at increasing radius lengths, and additionally with the canopy settings turned off. Consistent results across the three study sites showed that modeled

SWE matched observations most closely with canopy settings turned off. This suggests that within the SNOWPACK framework, the study sites are more accurately represented by open site conditions than forest clearings. All subsequent snow modeling in this study was conducted with canopy settings turned off.

2.4 Model forcings

The complete set of SNOWPACK model forcings was collected from the three study sites in Independence Creek Basin and additionally from a neighboring watershed, Upper Sagehen Creek Basin. The three study sites in the Independence Creek Basin are comparable to three Upper Sagehen Creek Basin weather stations in elevation,[3] they are similarly characterized by flat surfaces in forest gaps, and they feature vegetation alike in species composition and density. Like the study sites, the weather stations at Sagehen Creek are permanent installations. The period of record for Upper Sagehen Creek dates back to 1990. Model forcings collected in Independence Creek Basin were air temperature, precipitation and ground surface temperature. Model forcings collected in Upper Sagehen Creek Basin included relative humidity, ground surface temperature, windspeed, and incoming shortwave and longwave radiation. Data from both locations were combined to complete the SNOWPACK forcing dataset, taking place over the 'scenario anal-

[3] Upper Sagehen Creek Basin station elevations are 2350 *m* at the highest elevation, 2214 *m* at the middle elevation, and 1934 *m* at the lowest elevation weather station.

ysis period' from WYs 1981 to 2019. The 'calibration period' refers to the dataset constrained to WYs 2009 to 2019, and the 'validation period' to WYs 1981 to 2008.

Hourly air temperature at the three study sites was acquired for the calibration period from the NRCS Report Generator.[4] Known error in the dataset, from an incorrect algorithm applied to extended-range YSI air temperature sensors across the SNOTEL network, was corrected with the algorithm published in Harms et al. (2016). Monthly bias corrections of hourly data were made between the study sites to fill null values, data <-20°C and all data gaps. The forcing dataset was extended into the validation period with hourly NLDAS-2 data, bias corrected to each study site on a monthly basis.

Untrustworthy hourly totals of observed precipitation from rocket-style gauges can result from plugging, where snow freezes onto the sides and top of the gauge and is suspended above the antifreeze (J. Anderson, 2020). Error in the hourly totals were minimized with an algorithm that relies more heavily on quality-controlled, daily precipitation totals. Daily and hourly precipitation data were downloaded from the NRCS Report Generator. Daily values were dis-aggregated into hourly values using a scaling fraction, hourly total divided by daily total. This way, timing and relative magnitude of the hourly data were preserved. The calibration dataset was extended into the

[4] https://wcc.sc.egov.usda.gov/reportGenerator

validation period with NLDAS-2 data, bias corrected to each study site on a monthly basis.

For each calibration period forcing dataset, monthly bias corrections were developed using linear regressions of daily average observations from 2009-2019 between the study sites, those with the highest R^2 were used to fill data gaps. The dataset was extended into the validation period using downscaled NLDAS-2 data that was bias corrected to each study site on a monthly basis, using a linear regression. NLDAS data were collected from the grid cell encompassing the Truckee River Basin. The precipitation bias correction required two separate bias corrections be developed, one for the calibration period and another for the validation period, as trends in precipitation changed for our three study sites over the 40 years of the scenario analysis.

Hourly ground surface temperature for the calibration period was acquired from the NRCS Report Generator. The data were collected from the three study sites using a Hydraprobe Analog (2.5 Volt) at 2 in below the soil surface. Hourly relative humidity data for the calibration period was acquired from the Berkeley Sensor Database (sensor.berkeley.edu, BSD), the data were acquired with Vaisala HmP45C-L Temperature/Relative Humidity sensors located on meteorological towers at 100 ft above ground surface at the Sagehen Creek Basin stations. Hourly windspeed data for the calibration period was acquired from the BSD and collected with RM Young

Wind monitor 05103-L wind sensors located on the meteorological towers at 100 ft above ground level at the Sagehen Creek Basin stations. Hourly average incoming shortwave and longwave radiations starting in 2009 was downloaded from the BSD. The data were collected using a Campbell Scientific Li-Cor LI200X-L Pyranometer located at the lowest elevation station in Sagehen Creek Basin. Incoming shortwave radiation data were not available for the higher elevation weather stations in Sagehen Creek Basin.

To calibrate and validate SNOWPACK, SWE and snow depth observations were acquired for the Independence Creek SNOTEL stations from the NRCS Report Generator, where values published at midnight are quality controlled by NRCS staff. The quality controlled values were used to develop hourly datasets for SWE and snow depth. The midnight value was applied to each hour in the 24-hour period straddling the midnight timestamp. Streamflow data were acquired from the USGS' National Water Information System for USGS gauge 10343500 at Sagehen Creek north of Truckee, CA.

There are many definitions of a ROS event. The goal of an individual study usually determines the selection criteria for which ROS events are analyzed, with a large impact on study outcomes. In this study, ROS events are defined by periods of >5 *mm* total precipitation, > 5% precipitation as rain, and >5 *mm* starting SWE. A minimum of 24 hours was required between events and all events were capped at a maximum of 9 days (216 hours). Using this

criteria, a total of 71 ROS events were identified over the scenario analysis period.

Of those 71 events eight of the most extreme were chosen for further study, limiting the potential for redundancy in our results that might have been incorporated over a larger number of events. Extreme events with respect to warm air temperature and more or less wind were identified using a principle component analysis. Of that subsample of extreme events, eight events were chosen for their overall rain amount. Two events had approximately 300 *mm* of rain, '05 was a warm and windy event and '95 was less windy, and '86 had approximately 500 *mm* of rain. Two events had approximately 200 *mm* of rain, '96 was warm and windy, and '82 was warm and less windy. Two events had approximately 130 *mm* of rain, '17 was a warm and windy event and '83 was less windy, and '15 had approximately 60 *mm* of rain. All ROS events began 24 hours prior to the start of precipitation and continued until 24 hours after precipitation stopped, for a maximum duration of 9 days. At the end of one ROS event, a 24-hour period without precipitation buffered each event before the next began.

Model calibration and validation

Parameters and decisions in SNOWPACK allow the user to optimize performance by tailoring the model to specific environmental conditions at the

study site. Over 1,425 unique models, or combinations of parameters and decisions, were tested to optimize SNOWPACK's performance across our three study sites. The unique models incorporated parameterizations of percent rainfall (precipitation phase) and snow surface roughness values, as well as decisions pertaining to atmospheric stability, shortwave radiation absorption, new snow density, and albedo. Calibration included five unique aerodynamic roughness lengths (m): 0.0005, 0.001, 0.0075, 0.01 and 0.02, according to ranges specified for the Sierra Nevada in (Leydecker & Melack, 1999). Atmospheric stability was calibrated using 'MO_HOLSTAG' (Holtslag & De Bruin, 1988), the simple log-linear model 'MO_LOG_LINEAR' and 'MO_MICHLMAYR' (Stearns & Weidner, 2011; Michlmayr et al., 2008). Shortwave absorption was calibrated to both single- and multi-band schemes. The new snow density models used were 'LEHNING_NEW', 'ZWART' (Zwart, 2007), and 'PAHAUT' (Pahaut, 1976). Albedo parameterization models used were 'LEHNING_1', 'SCHMUCKI_GSZ' and 'SCHMUCKI_OGS' (Schmucki et al., 2014). Precipitation phase was calibrated using three air temperature thresholds, -2°C to 2°C, -1°C to 3°C, and 0°C to 4°C. Ranges were based on observations from an OTT Parsivel^2 laser disdrometer from the lowest elevation station in the Sagehen Creek Basin. The thresholds provided the lower and upper range for fully solid / fully liquid precipitation. Within the provided range, a linear transition was

assumed.

We performed a model calibration using a multi-objective function that focused specifically on ROS events. For 35 events between 2009 and 2019, we minimized the difference between observations and modeled predictions for (1) SWE at the start of the storm and (2) accumulated SWE losses over the course of the storm. The 10 top performing models over the multi-objective function were used to validate the model. Model validation was performed over a unique set of 135 ROS events from 1981 to 2008, and evaluated using the same multi-objective function from the calibration process.

Historical analysis and scenario analysis

ROS events chosen for the historical and scenario analysis are described in the 'Selection of events' section above. In both analyses, we use results from the SNOWPACK model, however the analyses differ with respect to antecedent snowpack conditions. Historical analysis ROS events were considered as the transpired. This is in contrast to the scenario analysis, where event meteorological forcing data (precipitation, air temperature, windspeed, etc.) for the eight most extreme events was held constant, while 40 different antecedent snowpacks varied. The 40 snowpacks occurred ev-

ery year on January 26, the average start date of all the ROS events.

3 Results

3.1 Historical ROS events and model performance

There was high variability in precipitation, rain fraction and SWE across 71 ROS events identified at S-1962 between WYs 1981 and 2019 (historical events). Average precipitation was 195 *mm*, average rain was 95 *mm*, and the average rain fraction was 0.49. The eight scenario analysis events, a subset of the historical events, were chosen for their extreme meteorological conditions (scenario events, Table 3.1). '86 had the most precipitation (779 *mm*) and the most rain (522 *mm*). '15 had the least precipitation (95 *mm*) and the least rain (72 *mm*). Rain fractions ranged from 0.67 to 0.91. Observed initial SWE averaged 403 *mm* across all events. Of the scenario analysis events, '95 had the highest initial SWE with 973 *mm* and '15 had the lowest initial SWE at 50 *mm*. Mean air temperature across all events averaged -1.1°*C*. Of the scenario analysis events, mean air temperature was highest for '15 (2.8°*C*) and lowest for '96 (-1.1°*C*). Mean event windspeeds increased with elevation, from 2.4 m/s to 3.1 m/s to 4.5 m/s. '86 had the highest mean windspeed across the watershed (4.7 m/s) and '95 had the lowest (2.3 m/s). Mean incoming short and longwave radiations, measured at S-1962, was 63 and 282 $Wm^{-}2$, respectively. Incoming shortwave was highest for '95 (93 $Wm^{-}2$) and lowest for '96 and '05 (37 $Wm^{-}2$). Incoming longwave

Table 3.1. Scenario analysis events dates and times

	'15	**'17**	**'83**	**'96**	**'82**	**'95**	**'05**	**'86**
Event start	2/5/15 1:00	2/5/17 1:00	11/14/83 21:00	12/28/96 11:00	2/11/82 19:00	3/7/95 2:00	12/24/05 15:00	2/10/86 19:00
Event end	22/10/15 22:00	2/13/17 1:00	11/21/83 4:00	1/4/97 2:00	2/17/82 4:00	3/15/95 1:00	1/1/06 18:00	2/17/86 19:00
Total event hours	141	192	151	159	129	191	192	168

was highest for '82 (306 $Wm^{-}2$) and lowest for '15 (278 $Wm^{-}2$).

The antecedent snowpack conditions, cold content, SWE, liquid water content and density, varied substantially across the historical and scenario analyses. A principle component analysis (PCA, Figure 3.1) compares the antecedent snowpack conditions of the historical events with those on January 26 each year that were used in the scenario analysis. The antecedent conditions of the historical analysis events were generally well bounded by the antecedent conditions of the scenario analysis events. The historical events tended to have more SWE, higher densities, and higher liquid water content than the scenario analysis events, but less cold content (Figure 3.5). For the highest elevation study site, antecedent SWE was approximately 160 mm less for the scenario analysis compared to historical conditions. The snowpack at each elevation study site was approximately 0.8 MJ colder for the scenarios than historical conditions.

Table 3.2. Historical analysis- observed event characteristics
(Meteorologic characteristic means are taken over the duration of the ROS event. The four horizontal rows for each meteorologic characteristic correspond to the study sites, the top row refers to S-1962, the second to S-2124, the third to S-2541, and the bottom to the watershed area-weighted site average. Meteorologic characteristics with only one row correspond to data collected at S-1962.)

	All events	**'15**	**'17**	**'83**	**'96**	**'82**	**'95**	**'05**	**'86**
Mean absolute humidity (%)	3.8, 3.4, 2.5, 3.2	4.1, 3.3, 2.2, 3.1	4.7, 3.9, 2.3, 3.6	3.7, 3.4, 2.2, 3.2	3.7, 3.5, 2.7, 3.5	4.2, 3.6, 2.7, 3.5	4.4, 4.0, 3.1, 3.8	3.8, 3.7, 2.9, 3.6	4.0, 3.5, 2.5, 3.4
Mean air temperature ($^{\circ}C$)	-1.0, -1.1, -2.3, -1.4	3.4, 2.8, 0.2, 2.2	2.0, 0.5, -1.7, 0.1	-1.1, -0.4, -1.9, -0.8	-1.8, -1.1, -1.4, -1.2	1.0, 0.8, 0.7, 0.8	1.8, 1.1, 0.1, 0.8	-1.0, 0.0, -0.3 -0.1	-0.3, -0.5, -1.0, -0.6
Antecedent SWE (mm)	253, 349, 760, 446	08, 08, 307, 110	363, 427, 1189, 673	38, 58, 178, 123	203, 257, 668, 446	234, 381, 1034, 563	455, 671, 1285, 891	13, 13, 338, 138	367, 487, 804, 560
Delta SWE (mm)	59, 82, 187, 107	15, 20, 390, 110	28, 61, 299, 73	33, 51, 145, 148	-31, 137, 211, 148	0, 33, 162, 63	0, 88, 252, 124	48, 84, 317, 140	246, 277, 602, 355
Mean wind velocity (ms^{-1})	2.5, 3.1, 4.6, 3.4	3.2, 2.6, 3.9, 2.9	3.5, 3.3, 5.0, 3.7	2.3, 3.0, 4.4, 3.3	2.6, 3.9, 5.9, 3.4	2.4, 3.0, 4.5, 3.3	1.5, 2.0, 3.0, 2.3	2.8, 3.7, 6.3, 4.3	3.4, 4.2, 6.4, 4.7
Mean incoming short wave radiation (Wm^{-2})[1]	63	75	56	53	37	54	93	37	61
Mean incoming long wave radiation (Wm^{-2})[1]	284	278	295	284	279	306	297	279	296

[1] Observed at S-1962 and applied to all study sites.

Table 3.3. Historical analysis- simulated event antecedent snowpack conditions
(S-1962, S-2124, S-2541, watershed area-weighted site average)

	All events	**'15**	**'17**	**'83**	**'96**	**'82**	**'95**	**'05**	**'86**
	-0.11,	0.00,	-0.07,	-0.02,	-0.1,	-0.58,	-0.05,	0.00,	-0.11,
	-0.10,	-0.02,	-0.11,	-0.02,	-0.02,	-0.31,	-0.06,	0.00,	-0.10,
	-0.14,	-0.05,	-0.25,	-0.03,	-0.20,	-0.66,	-0.08,	0.00,	-0.15,
Antecedent cold content (MJ)	-0.11	-0.03	-0.02	-0.02	-0.07	-0.41	-0.06	0.00	-0.11
	0.31,	0.0,	0.32,	0.16,	0.28,	0.30,	0.42,	0.32,	0.38,
	0.32,	0.20,	0.31,	0.16,	0.31,	0.32,	0.42,	0.32,	0.39,
	0.35,	0.34,	0.34,	0.20,	0.29,	0.34,	0.44,	0.36,	0.40,
Antecedent density ($kg/m3$)	0.33	0.23	0.32	0.17	0.31	0.33	0.43	0.33	0.39
	0.68,	0.00,	0.75,	0.93,	0.24,	0.00,	1.00,	2.03,	0.85,
	0.80,	0.00,	0.32,	0.00,	1.87,	0.00,	0.91,	1.05,	0.82,
	0.46,	0.23,	0.17,	0.86,	0.00,	0.00,	0.63,	2.49,	0.67,
Antecedent liquid water content (%)	0.72	0.06	0.30	0.25	1.3	0.00	0.85	1.45	0.79
	298,	00,	214,	34,	244,	377,	743,	113,	479,
	344,	13,	311,	32,	248,	430,	852,	60,	537,
	591,	165,	1006,	90,	238,	594,	1356,	117,	782,
Antecedent SWE (mm)	403	50	477	46	245	468	970	76	594
	-15	-39	-14	-15	-15	-9	-12	- 15	-11
	-16	-22	-14	-15	-18	-9	-11	-17	-11
	-13	-20	-8	-12	-17	-9	-10	-18	-9
Net longwave radiation (Wm^{-2})	-15	-23	-12	-14	-18	0	-11	-17	-10
	-3	-27	4	-3	0	0	-1	- 1	-3
	-5	-5	-2	-5	-1	-4	-3	-2	-8
	-16	-22	-25	-20	-14	-16	-11	-18	-30
Mean latent heat (Wm^{-2})	-8	-10	-7	-9	-9	-7	-5	-6	-13
	5	44	12	3	6	4	2	5	7
	7	7	8	5	12	7	3	10	11
	12	12	19	10	22	14	5	22	23
Mean sensible heat (Wm^{-2})	8	10	11	6	14	8	3	12	13

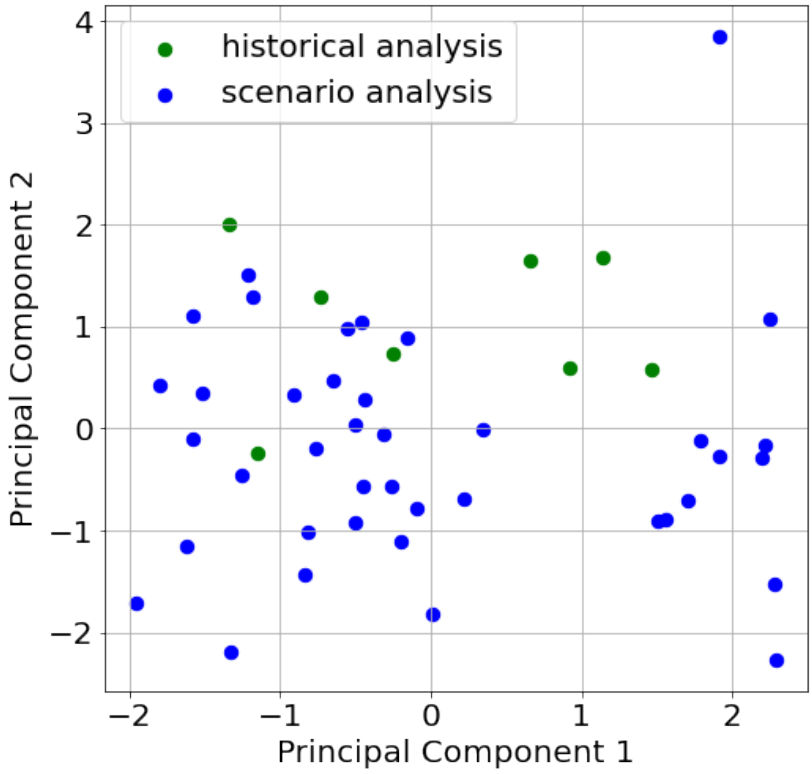

Figure 3.1. Antecedent snowpack conditions for the historical and scenario analyses. Principal component analysis shows the similarity between historical antecedent snowpack conditions and those used in the scenario analysis.

3.2 Calibrating and validating the SNOWPACK model

The calibration process identified the models that performed best over multiple points during an ROS event. The calibration considered 1,425 unique model decision or parameter combinations for snow surface roughness length, atmospheric stability scheme, shortwave radiation absorption scheme, new snow density, and albedo parameterization. The 10 highest performing models featured snow surface roughness lengths of 0.001 m and 0.0005 m,

Table 3.4. Historical analysis- event TWI response summary
(S-1962, S-2124, S-2541, watershed area-weighted site average)

	All events	**'15**	**'17**	**'83**	**'96**	**'82**	**'95**	**'05**	**'86**
Cumulative event rain (*mm*)	73, 89, 119, 95	76, 70, 78, 72	134, 137, 109, 130	101, 132, 177, 142	131, 191, 237, 199	145, 193, 338, 226	249, 264, 387, 293	244, 307, 356, 316	400, 453, 718, 522
Cumulative event TWI (*mm*)	59, 69, 86, 95	15, 70, 43, 61	148, 120, 31, 99	98, 129, 155, 134	113, 198, 228, 202	121, 176, 292, 202	268, 276, 373, 299	224, 303, 337, 308	402, 453, 678, 506
Cumulative event TWI/rain	0.62, 0.63, 0.55, 0.61	0.20, 1.00, 0.55, 0.86	1.10, 0.88, 0.28, 0.74	0.98, 0.97, 0.88, 0.95	0.87, 1.04, 0.97, 1.01	0.84, 0.91, 0.86, 0.90	1.08, 1.04, 0.96, 1.02	0.92, 0.99, 0.95, 0.97	1.01, 0.98, 0.95, 0.97

the 'MO_HOLSTAG' atmospheric stability scheme, single and multiband shortwave adsorption schemes, new snow density schemes 'ZWART', 'PAHAUT' and 'LEHNING_NEW', and the albedo parameterization scheme 'SCHMUCKI_OGS'.The model was calibrated to 35 events between 2009-2019 ('calibration period'). Calibration was performed using a high-quality,

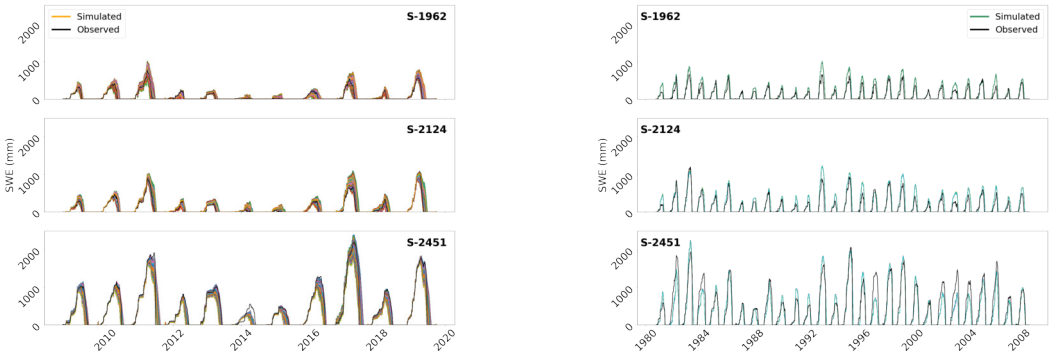

(a) (b)

Figure 3.2. Model performance. Annual SWE curves at the three study sites. Overall, simulated SWE from 1,450 unique versions of the SNOWPACK model (colored lines) show good agreement with observations (black line) over the calibration period, WYs 2009-2019. (a). Similarly, simulated SWE for the 10 highest performing models between the three sites (colored lines) show good agreement overall with observations (black line) over the validation period, WYs 1981-2008.

observed dataset collected from the study sites. The model was validated with 114 events between 1981-2008, ('validation period'). The model was simultaneously calibrated and validated to all three study sites, which spanned the watershed. The mean Nash-Sutcliffe efficiency for all calibration models on a daily basis at S-1962, S-2124 and S-2541 was 0.86, 0.83 and 0.91 (Hallouin, 2021). The calibration error percentages for RMSE of initial SWE was 9% at S-1962, 7% at S-2124, and 2% at S-2541. The calibration percentages for RMSE of accumulated SWE loss was 37% at S-1962, 32% at S-2124, and 125% at S-2541. The mean Nash-Sutcliffe efficiency for the ten validation models on a daily basis at S-1962, S-2124 and S-2541 was 0.54, 0.68 and 0.83. Validation model percentage errors for RMSE of initial SWE were 3%, 3%, and 2%, from the lowest to the highest elevation study site. Validation model percentage errors for RMSE of accumulated SWE loss were 7%, 12%, and 345%, from lowest to highest elevation study site. Calibration errors for RMSE of accumulated SWE loss were 30% and 20% higher than validation errors at the lower elevation study sites and 220% lower at the highest elevation study site. The difference in calibration and validation errors could be attributed to differences in data quality between the calibration and the validation periods, as well as the number of events considered (35 vs. 144).

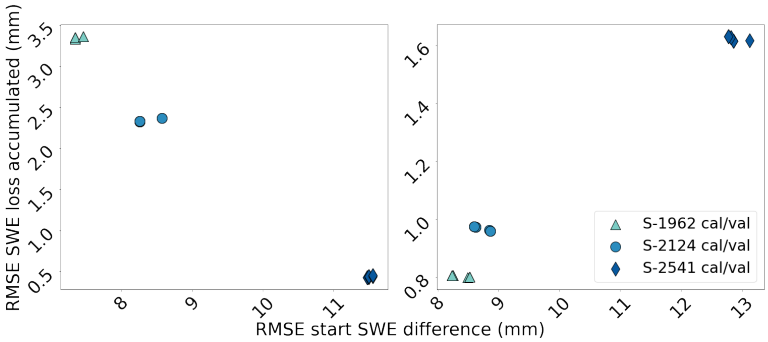

Figure 3.3. SNOWPACK calibration and validation. Performance of the 10 best models from the calibration (left panel) and the validation (right panel) at each study site. Model performance was assessed using a multi-objective function, RMSE of the difference between observed and simulated values of (1) SWE at the start of the event, and (2) the sum of SWE losses over duration of the event.

3.3 Historical analysis

Our results show two main positive relationships, (1) between the TWI/rain ratio and streamflow volume, and (2) between less negative modeled cold content and streamflow volume (Figure 3.4), which has implications for flooding. Ten events with TWI more than rain plot above the 1:1 line in Fig-

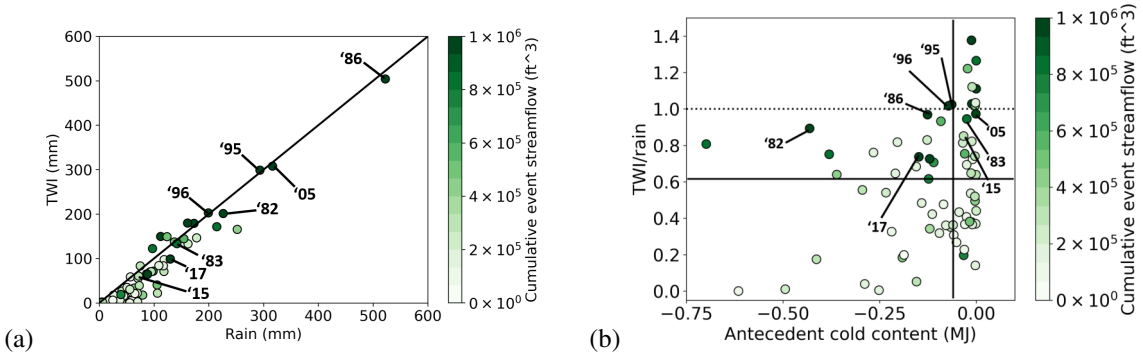

Figure 3.4. TWI response, cold content and stream flow. 71 historical ROS events between WYs 1981 to 2019 show a positive trend with a 1:1 line of rain and TWI. The largest rain events generate the largest TWI and also the greatest cumulative streamflow (a). Events with less negative cold content and TWI/rain close to 1, produce the largest streamflows. Black solid lines mark median values for each axis. A dotted, black line marks TWI/rain equal to 1 (b). Start dates correspond to the eight ROS events analyzed in the scenario analysis.

ure 3.4a. The three largest rain events are also the three largest TWI events, and plot on or almost on the 1:1 line. The majority of historical events begin with ripe snowpacks (Figure 3.4b). The largest TWI events '86, '05, '95 and '96, have TWI more than or equal to rain and little to no antecedent snowpack cold content. A positive trend, where events with TWI/rain near 1.0 and ripe snowpacks produce the largest streamflow volumes. '96 has TWI/rain>1.0 and produces the largest event streamflow, 21×10^7 ft^3 during the historical period. '95 also has TWI/rain>1.0 and generates 4×10^7 ft^3. '05 and ' 86 have TWI/rain near 1.0 and generate large streamflow volumes of 7.4×10^7 and 6.5×10^7 ft^3, respectively. Some events, however, have TWI/rain>1.0 and ripe snowpacks that produce smaller stream flows. This could be attributed to meteorological conditions, such as lower event windspeeds, or other antecedent conditions of the hydrological system like soil moisture and groundwater.

We find more rain at high elevations and TWI that increases with elevation during large historical ROS events (Figure 3.5). Mean cumulative event rain was 46 *mm* higher at S-2541 than S-1962, however the rain gradient with elevation was less steep for smaller events than larger events. The highest elevation experienced 2 *mm* more rain than the lowest elevation during '15 (the smallest event) and 318 *mm* during '86 (the largest event) (Table 3.4. TWI summed up over all events was 32% larger at S-2541 than S-1962, and

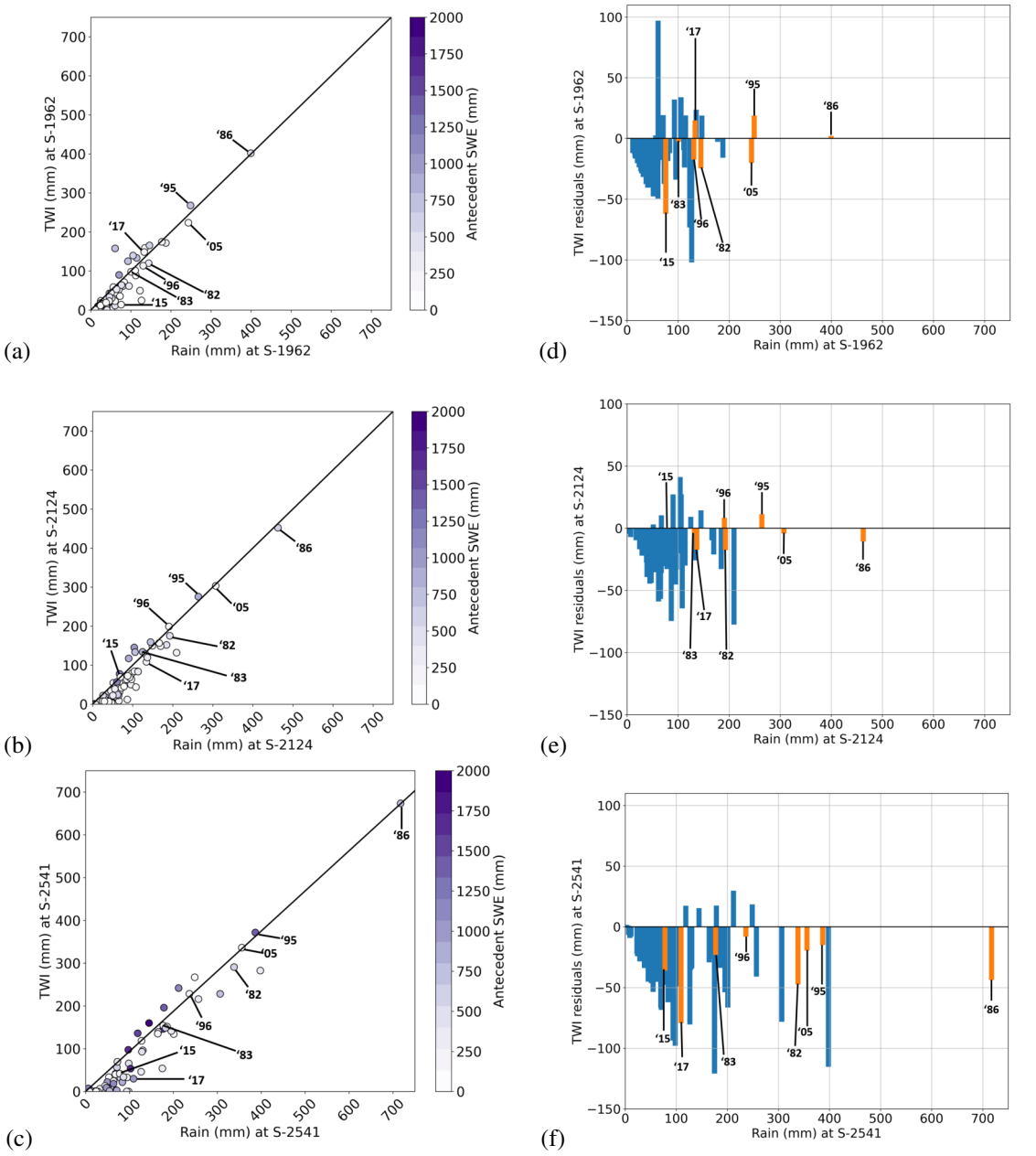

Figure 3.5. TWI with elevation. Left column: ROS events trend positively on a 1:1 line of rain and TWI at the highest, middle and low elevation study sites. Events are colored by inital SWE of the snowpack. ROS events that plot above the 1:1 line have the largest initial SWE for all historical events and across all study sites. Lower elevation study sites, S-1962 (a) and S-2124 (b), have less initial SWE than S-2541 (c). Right column: TWI residuals, the difference between TWI and rain, at the highest, middle and lowest elevation study sites. TWI residuals greater than zero correspond to events with more TWI than rain. Positive TWI residuals are more common and larger at the lower elevation sites (d) and (e) than at (f), the highest elevation site. Events labeled with start dates correspond to the eight events analyzed in the scenario analysis.

20% larger than S-2124. For ’86, the largest TWI response, S-2541 contributed the most TWI (678 *mm*) to the watershed, whereas the S-2124 and S-1962 contributed less, 453 *mm* and 402 *mm* TWI, respectively. Adjusted for the size of the ’86 event, the TWI/rain ratio decreases with elevation, from 0.95 at S-2541 to 1.01 at S-1962, suggesting that for the same amount of rain S-1962 would produce more TWI. Potentially, some ROS events in the northern Sierra are temperature inverted, whereby S-2541 experiences a greater rain precipitation than S-2124 or S-1962. ’17, a smaller event, had more rain at the low elevation than the high elevation, this generated the highest TWI/rain ratio of any site for all events. Residuals of TWI and the 1:1 line, particularly residuals<0, show that S-1962 and S-2124 retain less rain than S-2541, by 43% and 35% respectively (Figure 3.5). Large initial SWE at higher elevations may facilitate liquid water storage through freezing and/or refreezing.

3.4 Scenario analysis

Results of the scenario analysis show that different antecedent conditions lead to a wide range in TWI/rain. Some events switch from TWI/rain >1 to <1 and others are largely different from the historical ratio. With meteorological conditions held constant for each event, TWI and TWI/rain responses were the result of differences in antecedent snowpack only 3.6c). While TWI increases linearly with rain input, TWI/rain ratios increase in a

horseshoe pattern, where events with mean cumulative event rain >200 *mm* and <300 *mm* have the largest TWI/rain ratios. Of the eight scenario modelling events, ’82 and ’95 had mean TWI/rain >1, 1.01 and 1.00 respectively. Mean TWI/rain for ’82 switches from ≤ 1 historically to ≥ 1 in the scenarios, with a 0.11 difference in mean TWI/rain (*unitless*). There is TWI/rain ≥ 1 for 21 out of 40 of the ’82 scenarios and for 25 out of 40 of the ’95 scenarios. 15 out of 40 ’96 scenarios have TWI/rain ≥ 1, however the event mean is lower than 1. The TWI/rain scenario response encompassed the historical response for all events, except for ’86. The scenario response spread for TWI/rain generally decreased with mean cumulative event TWI/rain ratios and event size. ’15, the smallest event, had the lowest mean TWI/rain ratio (0.64) and the mostly highly variable TWI/rain response (82%). ’83, the third smallest event, had 74% variability in TWI/rain responses. The four events with the highest mean cumulative event TWI/rain ratios had the four lowest TWI/rain response variabilities. While the pattern for TWI/rain response varied with size of the event, less negative cold content snowpacks consistently generated more TWI and higher TWI/rain ratios across all events.

Cold content is the most important antecedent condition for predicting TWI for the eight extreme events in the scenario analysis. A multiple linear regression analysis (MLR) with 0.75 average R^2 explains the variance in TWI

Table 3.5. Scenario analysis- simulated event antecedent snowpack conditions
(S-1962, S-2124, S-2541, watershed area-weighted site average)

	All events
Mean antecedent cold content (MJ)	-0.19, -0.19, -0.23, -0.20
Mean antecedent density ($kg/m3$)	0.28, 0.29, 0.32, 0.30
Mean antecedent liquid water content (%)	1.0, 0.6, 0.37, 0.57
Mean antecedent SWE (mm)	252, 271, 427, 308

Table 3.6. Scenario analysis- event TWI response summary
(S-1962, S-2124, S-2541, watershed area-weighted site average)

	'15	**'17**	**'83**	**'96**	**'82**	**'95**	**'05**	**'86**
Mean cumulative event rain (mm)	76, 70, 78, 72	134, 137, 109, 130	101, 132, 177, 142	131, 191, 237, 199	145, 193, 338, 226	249, 264, 387, 293	244, 307, 356, 316	400, 453, 718, 522
Mean cumulative event TWI (mm)	65, 49 32, 46	143, 133, 59, 115	107, 72, 128, 87	108, 186, 228, 193	148, 196, 331, 227	255, 270, 361, 292	202, 275, 295, 277	339, 376, 556, 419
Mean cumulative event TWI/rain	0.86, 0.71, 0.41, 0.64	1.07, 0.97, 0.54, 0.86	0.71, 0.81, 0.72, 0.78	0.83, 0.97, 0.96, 0.96	1.03, 1.02, 0.98, 1.01	1.03, 1.02, 0.93, 1.00	0.83, 0.89, 0.83, 0.87	0.85, 0.81, 0.78, 0.80
Variability of cumulative event TWI/rain responses (%)	82	45	74	26	26	18	21	75[1]

[1] An outlier for this event increases the variability.

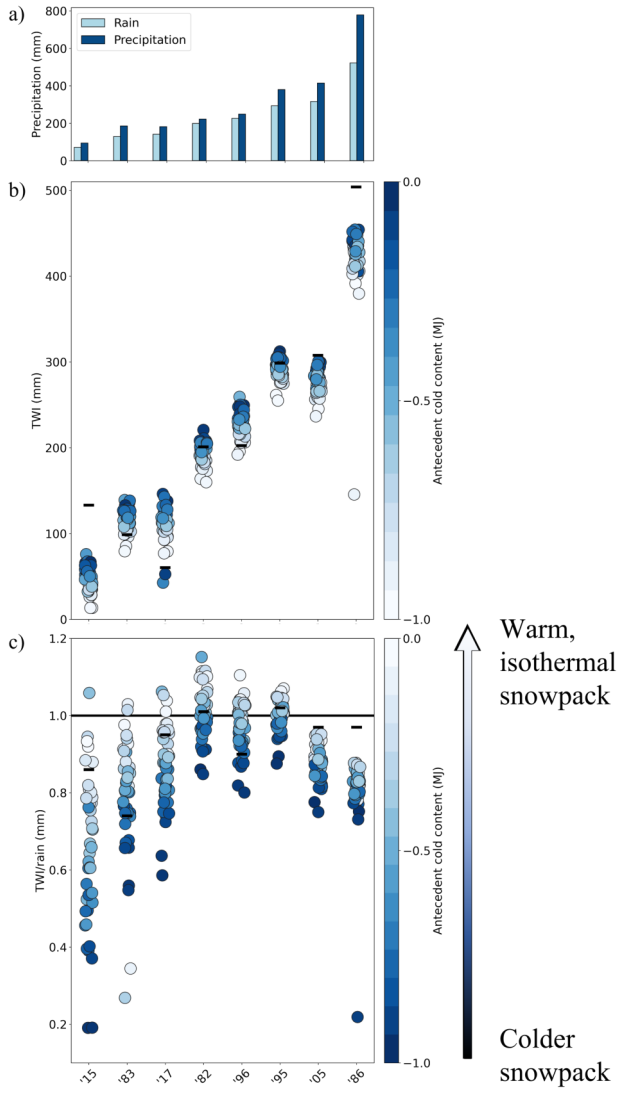

Figure 3.6. Variability in TWI and TWI/rain for eight large ROS events. Eight of the largest ROS events in the Sagehen Creek catchment increase in rain amount from left to right. A bar chart compares cumulative event rain and precipitation (a). These events show high variability in TWI (b) and TWI/rain (c) over realistic, mid-winter antecedent snowpack conditions. Events are colored by antecedent cold content of the snowpack and observed values are denoted by black bars.

due to antecedent snowpack conditions (Figure 3.7 and associated table). Beta coefficients show generally logical relationships between antecedent conditions and TWI response. For most events, greater antecedent cold content (warmer snowpack) and greater liquid water content lead to an increase in cumulative event TWI, whereas antecedent SWE and density have the opposite response. It is expected that interrelated factors such as SWE and density would have the same effect on the snowpack, however it is non-intuitive that greater antecedent density decreases TWI. Higher density snowpacks are typically indicative of riper snowpack conditions, requiring less energy to melt than a low density snowpack. Therefore, the density result is surprising, however, the magnitude of the mean response (-0.01) is small. Also surprising is the large difference in the magnitude for cold content and liquid water content beta coefficients, since these two factors are also interrelated. MLR results show that a 1 MJ increase in antecedent cold content would generate 0.73 mm greater TWI, which is 69% more influential for TWI response than a 1% increase in antecedent liquid water content, the second most influential factor. Cold content is least influential for '86, the largest ROS event, which can be explained by the low event R^2 and the scenario outlier. The low R^2 for '83 brings into question the strong influence of liquid water content on this event more so than all other events.

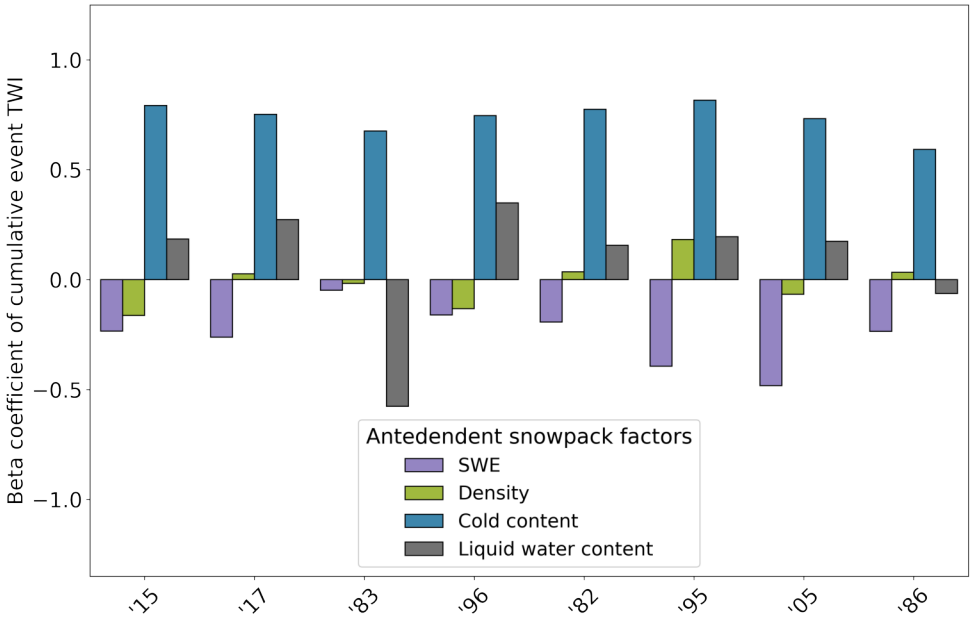

	Antecedent snowpack factor	**Mean for all events**	**'15**	**'17**	**'83**	**'96**	**'82**	**'95**	**'05**	**'86**
Beta coefficient	SWE	-0.19	-0.23	0.26	-0.05	-0.16	-0.19	-0.39	-0.48	-0.24
	Density	-0.01	-0.16	0.03	-0.02	-0.13	0.04	0.18	-0.07	0.03
	Cold content	0.74	0.79	0.75	0.68	0.75	0.78	0.82	0.73	0.59
	Liquid water content	0.23	0.19	0.27	-0.58	0.35	0.16	0.20	0.18	-0.06
R^2		0.76	0.80	0.87	0.55	0.93	0.77	0.91	0.91	0.35

Figure 3.7. Antecedent cold content predicts TWI for eight large ROS events. A multiple linear regression (MLR) analysis, mean R^2 >0.75, shows that cold content is the most influential antecedent snowpack factor over SWE, density, and liquid water content, in predicting TWI for eight large ROS events with variable mid-winter antecedent snowpack conditions. ROS event sizes order from left to right. Table shows numerical results from the MLR, beta coefficient and R^2 values for each of the eight large events.

4 Discussion

ROS events with greater rainfall and higher TWI/rain ratios cause the largest floods in the Sagehen Creek catchment, an important drainage to the Truckee River. The large ROS events used in this study correspond to extreme events that challenged northern Sierra Nevada water management. For example, the 12/28/96 event was the 1997 'New Year's Day Flood', which is estimated to have caused $540 million in damages at the time (USGS, 1997) in the downstream Truckee Meadows. The '17 ROS event triggered the disaster at the Oroville Dam emergency spillway just north and east of Sagehen Creek. As expected, large amounts of rain are correlated with large TWI response during these flood events. However, we show that the amount of TWI can vary considerably across realistic antecedent snowpack conditions.

The variability in TWI has important implications for the historical context of these large flood events. For example, the 'New Year's Day Flood' ('96) event had a TWI/rain ratio closer to 1 and in the upper quartile of potential TWI response compared to the antecedent conditions in the scenario analysis, which is consistent with this being a large large flood event in the Truckee River. Conversely, the '17 event had lower rainfall and also lower

TWI to rain ratio that was near the median TWI response compared to the scenario analysis (Figure 3.6), which led to smaller downstream flooding effects in the Truckee Basin (Kozlowski & Ekern, n.d.). In general the scenario analysis captures the true historical response, however the '86 event has greater TWI than the range of variability considered using January 26 conditions each year. While our analysis of TWI simplifies many of the other key variables causing large floods, like rain snow elevation, orographic precipitation effects, and antecedent soil and groundwater conditions, it does show that antecedent snowpack conditions can play a large role in determining the amount of water available to become runoff and streamflow.

Historical analysis and a scenario-based scenario analysis confirm the importance of cold content in the amount of TWI and the flood potential from a given amount of rainfall in our study catchment. Over the period 1989 to 2019, ROS events with the largest TWI response had ripe snowpacks, with isothermal snowpacks producing more TWI than rain (Figure 3.4b), implying drainage of snowmelt or liquid water in the snowpack. In agreement with Trubilowicz & Moore (2017) and Würzer et al. (2016), in Figure 3.6b and c, we show the amplifying and dampening affects of snowpack on TWI, but update this conceptual model to include the consequences of an elevation gradient in predicting catchment-scale TWI response.

In our study catchment, ROS events with historical rainfall ≤ 130 *mm* had

storage of liquid water at the highest elevation that dampens the catchment-scale TWI response, except in the most extreme ripe antecedent conditions (Figure 3.5c and f). This is consistent with anecdotal evidence and measurements (Table 3.4) during the '17 event, when TWI at the highest elevations was less than 30 percent of incoming rainfall. We term these types of events as 'high elevation dampened ROS' and they are accentuated by smaller rainfall, steeper precipitation (orographic) gradients in snowpack and cold content (i.e. more cold snow at high elevation), as well as a higher gradients in rainfall with increasing elevation. The magnitude of TWI/rain response is greatest for events with rainfall >150 *mm* and <300 *mm*, events where cumulative TWI is greater than rainfall from melting snow or water storage at low elevations and high elevation snowpacks store relatively little rainfall. We term these storms 'low elevation melt ROS' events (Figure 3.5) and they are most likely to occur when 'high elevation dampened' events are less likely, meaning less cold content, less steep snowpack gradients with elevation, and a more 'upside-down' precipitation gradient with more precipitation (and energy inputs) at lower elevations. An interesting example is the '95 and '05 events that have similar amounts of rain (293 and 316 *mm*), but very different TWI/rain ratios of 1.00 and 0.87, respectively, due to larger overall energy inputs (Table 3.2) and higher solar insolation during the '95 event.

Lastly, there is some evidence of the highest rainfall event ('86) also having TWI/rain ratios <1, despite having more rainfall and overall TWI. We term these events as 'all elevations draining' and they would tend to occur during the largest rain events when cold snowpack conditions and steep orographic gradients exist. We assume that this occurs because liquid water cannot be stored in the snow matrix, but there is insufficient energy to melt the snowpack. Given '86 is such a unique rainfall event (~40 percent larger than the next largest event), it may be possible to see large events like the '86 event but with active melt at lower elevations, but our historically-driven analysis for 39 years did not observe that type of storm. Because snowpack response to different storm events is rarely measured at a high temporal resolution (sub-hourly), efforts like this requires a skillful physical model and accurate forcing and validation datasets.

Modeling ROS processes is extremely difficult requiring a number of assumptions that underlie the inferences made about ROS flood risk. The SNOWPACK model has been used with different cold contents (Jennings, Kittel, & Molotch, 2018), different snowpack depths (Rasmus et al., 2007), wet (Yamaguchi, Sato, & Michael Lehning, 2004) and dry snowpacks (Lundy et al., 2001), high elevation and low elevation snowpacks (Wever, Jonas, et al., 2014), in the forest (Watts et al., 2016), and in the Sierra Nevada mountains (Musselman, Molotch, et al., 2012). While the physics of the

model are sophisticated compared to most land surface models, i.e. applying the RE, SNOWPACK does not consider several important processes like preferential flowpaths that are documented during ROS events. Preferential flowpaths would increase TWI by increasing the vertical hydraulic conductivity and avoid layers of negative cold content that would have otherwise frozen liquid water into an ice layer (Humphrey, Harper, & Pfeffer, 2012). For larger ROS events, preferential flow paths become increasingly important, efficiently carrying more water down though the snowpack (Würzer et al., 2016). In a comparison of a SNOWPACK initiated with a simple bucket-type water balance scheme and a full application of the RE, Wever, Jonas, et al. (2014) found that for sites with frequent melt, mid-winter melt, and/or preferential flow paths, both schemes produced less runoff than was measured, however, the full RE showed slightly better agreement with observations. An advanced treatment of SNOWPACK using the 'dual domain approach' proposed by Wever, Würzer, et al. (2016) could improve preferential flow and ice layer formation, but requires additional calibration in often data sparse settings. Model forest clearings of >30 m in diameter as open areas, which minimized the potential effects of shading from shortwave radiation, lessened wind speeds and turbulent fluxes (Burns et al., 2014), and minimized forest debris accumulation onto the snowpack (Gleason, Nolin, & Roth, 2013). A simple extension of this work would be to understand

the role of forest cover, which is extensive in the study area, in modulating the role of cold content in TWI variability. Our scenario analysis only considered the conditions on January 26 to try to give a realistic range of conditions. Realistically, however, the conditions on January 26 may have been primed for melt or resistance to melt in unexpected ways. The influence of consecutive ROS events (White et al., 2019) or other catalyst meteorological events (Kroczynski, 2004), like uncharacteristically warm or cold air temperatures, may have set up the snowpack prior to January 26 in an unusual way. It may be possible to limit these kinds of confounding variables using SNOWPACK or similar calibrated models to understand which snowpack conditions could produce the most extreme ROS response and how that might evolve with climate change.

Our work shows the potential importance of modeling and monitoring antecedent snowpack conditions for operational ROS streamflow forecasting and their interactions with meterological characteristics of the event. This study highlights the influence of antecedent conditions, specifically cold content, on TWI response during ROS events and associated implications for flooding. In particular, our model results show that cold content can increase or decrease the TWI response by 20%-30% from the mean response during extreme ROS events of very different rainfall and energy conditions, which is substantial if that variability is translated directly to

streamflow response. The relatively large events of 150-300 *mm* of rainfall will be important to predict for operational purposes because a switch of TWI by 30 percent could be the difference between a hazardous flood and one that is below the flood stage. Conversely, the very largest events may be less important to predict because the flood warnings will likely be made either way, and in the case of the 1986 storm the variability in TWI caused by antecedent conditions was lower. The operational flood forecast model SNOW-17 operates on a simplified energy-balance framework that tracks cold content but not other key variables like density and is poorly validated (E. Anderson, 2006). Because the 'low and mid elevation melt' scenario is the most problematic for flood forecasting, the antecedent conditions for these events seem particularly important to predict or measure. Weather monitoring stations, such as the NRCS SNOTEL stations, measure SWE and depth of the snowpack, but not density, liquid water content, or cold content, which largely require in-person measurement by-hand (Techel & Pielmeier, 2011) or poorly validated, new sensing technologies. Additional monitoring of cold content could be used directly in model tuning efforts, as well as validation of different models. Future comparisons of TWI response of SNOWPACK versus SNOW-17 across elevation gradients could illuminate potential improvements to the operational models.

The ability to forecast ROS associated stream and river floods under a chang-

ing climate will depend on our ability to predict antecedent conditions of the snowpack and how they interact with extreme meteorological events. Increasing water demand driving changes in reservoir management to release water based on hydrological forecasts of reservoir inflows. Changes in atmospheric river conditions that generate ROS events and potential increases to rainfall amounts and intensity have been predicted. Combined with increasing 'weather whiplash' that swings between droughts and floods, climate change will place additional pressure on water managers to effectively predict winter flood events. Climate change is expected to decrease SWE and cold content, which would increase TWI according to our results, with everything else equal. However, two key questions remain for forecasters: 1. What causes the dampening and draining response and how will future climate change that occurrence of those events? and 2. Will there be more very large events like 1986, but with sufficient energy to melt part of the snowpack and thereby generate even larger flood events? If the upper elevation snowpack began to melt and contribute additional water in a future climate that could heighten the effects on flooding beyond what was showed in our historical and scenario analyses. In contrast, if lower elevation areas become partially or completely snow free that will tend to lessen the effects of low and mid elevation melt (Nolin & Daly, 2006; Musselman, Lehner, et al., 2018). Despite the uncertainty of long-term forecasts, flood forecasters

are in the unenviable situation of using a suite of meteorological ensembles but a deterministic (and simplistic) hydrological model. Consequently, we suggest there is potential for immediate impact on operational modeling by better representing antecedent conditions like cold content. The potential to increase our modeling and measuring ability of high elevation snowpack appears to be critical for effectively constraining upland hydrological response to ROS events in this part of the Sierra Nevada.

5 Conclusions

Climate change and water demands will make streamflow prediction during ROS events even more important. However, this study shows that antecedent snowpack conditions that are rarely measured, like cold content and liquid water content, are likely critical to predicting the TWI response that is explanatory of the large stream flooding events. Large rains and ripe snowpacks produce the largest floods events, and with climate change, larger rains and riper snowpacks will produce even larger floods. Perhaps, the future holds larger floods than any flood in the last forty years. Larger inflows to reservoirs may trigger reservoir floods potentially more devastating than the 2017 Oroville Dam incident. Reservoir managers will be required to keep a safe amount of empty winter storage at all times. Climate change in the US West will require even higher levels of complex water resources

management and constraints to an already limited water supply.

6 References

Anderson, Eric (2006). *Snow Accumulation and Ablation Model-SNOW-17*. Tech. rep.

Anderson, Jeff (2020). *Personal communication*. Reno, Nevada.

Bartelt, P & M Lehning (2002). "A physical SNOWPACK model for the Swiss avalanche warning. Part I: numerical model". In: *Cold Regions Science and Technology* 35, pp. 123–145.

Brekke, L. et al. (2014). "A Vision for Future Observations for Western U.S. Extreme Precipitation and Flooding". In: *Journal of Contemporary Water Research & Education*. DOI: 10.1111/j.1936-704x.2014.03176.x.

Broxton, P. D. et al. (2015). "Quantifying the effects of vegetation structure on snow accumulation and ablation in mixed-conifer forests". In: *Ecohydrology* 8.6, pp. 1073–1094. ISSN: 19360592. DOI: 10.1002/eco.1565.

Burns, Sean P. et al. (2014). "Snow temperature changes within a seasonal snowpack and their relationship to turbulent fluxes of sensible and latent heat". In: *Journal of Hydrometeorology* 15.1, pp. 117–142. ISSN: 1525755X. DOI: 10.1175/JHM-D-13-026.1.

Delaney, Chris J. et al. (2020). "Forecast Informed Reservoir Operations Using Ensemble Streamflow Predictions for a Multipurpose Reservoir in Northern California". In: *Water Resources Research* 56.9. ISSN: 19447973. DOI: 10.1029/2019WR026604.

Dettinger et al. (2004). "Simulated Hydrologic Responses To Climate Variations". In: *Climatic Change* 62, pp. 283–317. ISSN: 0165-0009.

Dozier, J et al. (1989). *Snow, snowmelt, rain, runoff, and chemistry in a Sierra Nevada watershed*. URL: http://o3.arb.ca.gov/research/apr/past/a6-147-32a.pdf.

Garvelmann, Jakob, Stefan Pohl, & Markus Weiler (2015). "Spatio-temporal controls of snowmelt and runoff generation during rain-on-snow events in a mid-latitude mountain catchment". In: *Hydrological Processes*. ISSN: 10991085. DOI: 10.1002/hyp.10460.

Gleason, Kelly E., Anne W. Nolin, & Travis R. Roth (2013). "Charred forests increase snowmelt: Effects of burned woody debris and incoming solar radiation on snow ablation". In: *Geophysical Research Letters* 40.17, pp. 4654–4661. ISSN: 19448007. DOI: 10.1002/grl.50896.

Glossary of Meteorology: Atmospheric River (2018). URL: https://glossary.ametsoc.org/wiki/Atmospheric_river.

Golding, L & Robert H Swanson (1986). “Study • rea”. In: 22.13, pp. 1931–1940.

Gouttevin, I. et al. (2015). “A two-layer canopy model with thermal inertia for an improved snowpack energy balance below needleleaf forest (model SNOWPACK, version 3.2.1, revision 741)”. In: *Geoscientific Model Development* 8.8, pp. 2379–2398. ISSN: 19919603. DOI: 10.5194/gmd-8-2379-2015.

Guan, Bin et al. (2016). “Hydrometeorological characteristics of rain-on-snow events associated with atmospheric rivers”. In: *Geophysical Research Letters* 43.6, pp. 2964–2973. ISSN: 19448007. DOI: 10.1002/2016GL067978.

Hallouin, Thibault (2021). *hydroeval*. DOI: 10.5281/zenodo.4709652. URL: https://github.com/ThibHlln/hydroeval/tree/v0.1.0.

Harms, Deborah S. et al. (2016). “Comparing a SNOTEL Extended-Range Air Temperature Sensor and Equations to a NIST-Certified Sensor in an Environmental Chamber”. In: *84th Annual Western Snow Conference*, pp. 123–128.

Hatchett, Benjamin J. et al. (2017). “Winter snow level rise in the Northern Sierra Nevada from 2008 to 2017”. In: *Water (Switzerland)*. ISSN: 20734441. DOI: 10.3390/w9110899.

Henn, Brian et al. (2020). “Extreme Runoff Generation From Atmospheric River Driven Snowmelt During the 2017 Oroville Dam Spillways Incident”. In: *Geophysical Research Letters* 47.14, pp. 1–11. ISSN: 19448007. DOI: 10.1029/2020GL088189.

Holtslag, A. A. M. & H. A. R. De Bruin (June 1988). “Applied Modeling of the Nighttime Surface Energy Balance over Land”. In: *Journal of Applied Meteorology* 27.6, pp. 689–704. ISSN: 0894-8763. DOI: 10.1175/1520-0450(1988)027<0689:AMOTNS>2.0.CO;2. URL: http://journals.ametsoc.org/doi/10.1175/1520-0450(1988)027%3C0689:AMOTNS%3E2.0.CO;2.

Humphrey, Neil F., Joel T. Harper, & W. Tad Pfeffer (2012). “Thermal tracking of meltwater retention in Greenland’s accumulation area”. In: *Journal of Geophysical Research: Earth Surface* 117.1, pp. 1–11. ISSN: 21699011. DOI: 10.1029/2011JF002083.

Jennings, Keith S., Timothy G.F. Kittel, & Noah P. Molotch (2018). “Observations and simulations of the seasonal evolution of snowpack cold content and its relation to snowmelt and the snowpack energy budget”. In: *Cryosphere* 12.5, pp. 1595–1614. ISSN: 19940424. DOI: 10.5194/tc-12-1595-2018.

Kattelmann, Richard (1996). *Flooding from rain-on-snow events in the Sierra Nevada*. Tech. rep. 239.

Kim, Jinwon et al. (2013). “Effects of atmospheric river landfalls on the cold season precipitation in California”. In: *Climate Dynamics* 40.1-2, pp. 465–474. ISSN: 09307575. DOI: 10.1007/s00382-012-1322-3.

Klos, P. Zion, Timothy E. Link, & John T. Abatzoglou (July 2014). “Extent of the rain-snow transition zone in the western U.S. under historic and projected climate”. In: *Geophysical Research Letters* 41.13, pp. 4560–

4568. ISSN: 00948276. DOI: 10.1002/2014GL060500. URL: http://doi.wiley.com/10.1002/2014GL060500.

Knowles, Noah, Michael D. Dettinger, & Daniel R. Cayan (2006). "Trends in snowfall versus rainfall in the western United States". In: *Journal of Climate* 19.18, pp. 4545–4559. ISSN: 08948755. DOI: 10.1175/JCLI3850.1.

Kozlowski, Dan & Mike Ekern (n.d.). *Heavy Precipitation Event Southwest Oregon, Northern California, and Western Nevada December 26, 1996 - January 3, 1997*. Tech. rep. California Nevada River Forecast Center. URL: https://www.cnrfc.noaa.gov/storm_summaries/jan1997storms.php.

Kroczynski, Scott (2004). "A comparison of two rain-on-snow events and the subsequent hydrologic responses in three small river basins in central Pennsylvania". In: *Eastern Region Technical Attachment* 2004-04, p. 21. URL: https://repository.library.noaa.gov/view/noaa/6656.

Lehning, M, P Bartelt, B Brown, & C Fierz (2002). "A physical SNOWPACK model for the Swiss avalanche warning Part III: Meteorological forcing, thin layer formation and evaluation". In: *Cold Regions Science And Technology* 35.3, pp. 169–184.

Lehning, M, P Bartelt, B Brown, C Fierz, & P Satyawali (2002). "A physical SNOWPACK model for the Swiss avalanche warning Part II. Snow microstructure". In: *Cold Regions Science and Technology* 35.3, pp. 147–167. URL: papers2://publication/uuid/A55AB87D-E628-4EF3-90EA-E523090892DE.

Leydecker, Al & John M. Melack (1999). "Evaporation from snow in the central Sierra Nevada of California". In: *Nordic Hydrology* 30.2, pp. 81–108. ISSN: 00291277. DOI: 10.2166/nh.1999.0005.

Luce, C. H. & D. G. Tarboton (2009). "Evaluation of alternative formulae for calculation of surface temperature in snowmelt models using frequency analysis of temperature observations". In: *Hydrology and Earth System Sciences Discussions* 6.3, pp. 3863–3890. ISSN: 1812-2116. DOI: 10.5194/hessd-6-3863-2009.

Lundy, Christopher C. et al. (2001). "A statistical validation of the snowpack model in a Montana climate". In: *Cold Regions Science and Technology* 33.2-3, pp. 237–246. ISSN: 0165232X. DOI: 10.1016/S0165-232X(01)00038-6.

Marks, Danny, John Kimball, et al. (1998). "The sensitivity of snowmelt processes to climate conditions and forest cover during rain-on-snow: a case study of the 1996 Pacific Northwest flood". In: *Hydrological Processes* 12.10-11, pp. 1569–1587. ISSN: 08856087. DOI: 10.1002/(SICI)1099-1085(199808/09)12:10/11<1569::AID-HYP682>3.0.CO;2-L.

Marks, Danny & Adam Winstral (2001). "Comparison of snow deposition, the snow cover energy balance, and snowmelt at two sites in a semiarid mountain basin". In: *Journal of Hydrometeorology* 2.3, pp. 213–227. ISSN: 1525755X. DOI: 10.1175/1525-7541(2001)002<0213:COSDTS>2.0.CO;2.

Mazurkiewicz, Adam B., David G. Callery, & Jeffrey J. McDonnell (2008). “Assessing the controls of the snow energy balance and water available for runoff in a rain-on-snow environment”. In: *Journal of Hydrology* 354.1-4, pp. 1–14. ISSN: 00221694. DOI: 10.1016/j.jhydrol.2007.12.027.

Michlmayr, Gernot et al. (Sept. 2008). “Application of the Alpine 3D model for glacier mass balance and glacier runoff studies at Goldbergkees, Austria”. In: *Hydrological Processes* 22.19, pp. 3941–3949. ISSN: 08856087. DOI: 10.1002/hyp.7102. URL: https://onlinelibrary.wiley.com/doi/10.1002/hyp.7102.

Musselman, Keith N., Martyn P. Clark, et al. (2017). “Slower snowmelt in a warmer world”. In: *Nature Climate Change* 7.3, pp. 214–219. ISSN: 17586798. DOI: 10.1038/nclimate3225.

Musselman, Keith N., Flavio Lehner, et al. (2018). *Projected increases and shifts in rain-on-snow flood risk over western North America*. DOI: 10.1038/s41558-018-0236-4.

Musselman, Keith N., Noah P. Molotch, et al. (2012). “Improved snowmelt simulations with a canopy model forced with photo-derived direct beam canopy transmissivity”. In: *Water Resources Research* 48.10, pp. 1–21. ISSN: 00431397. DOI: 10.1029/2012WR012285.

Nolin, Anne W. & Christopher Daly (2006). “Mapping ”at risk” snow in the Pacific Northwest”. In: *Journal of Hydrometeorology* 7.5, pp. 1164–1171. ISSN: 1525755X. DOI: 10.1175/JHM543.1.

Ohba, Masamichi & Hiroaki Kawase (2020). “Rain-on-Snow events in Japan as projected by a large ensemble of regional climate simulations”. In: *Climate Dynamics* 55.9-10, pp. 2785–2800. ISSN: 14320894. DOI: 10.1007/s00382-020-05419-8. URL: https://doi.org/10.1007/s00382-020-05419-8.

Pahaut, Edmond (1976). *La metamorphose des cristaux de neige (Snow crystal metamorphosis)*. Meteo France.

Rasmus, Sirpa et al. (2007). “Validation of the SNOWPACK model in five different snow zones in Finland”. In: *Boreal Environment Research* 12.4, pp. 467–488. ISSN: 12396095.

Richards, L. A. (1931). “Capillary conduction of liquids through porous mediums”. In: *Journal of Applied Physics* 1.5, pp. 318–333. ISSN: 01486349. DOI: 10.1063/1.1745010.

Rössler, O et al. (2013). *Retrospective analysis of a non-forecasted rain-on-snow flood in the Alps – a matter of model-limitations or unpredictable nature?* Vol. 10. 10, pp. 12861–12904. ISBN: 1012861201. DOI: 10.5194/hessd-10-12861-2013.

Santer, B. D. et al. (2007). “Identification of human-induced changes in atmospheric moisture content”. In: *Proceedings of the National Academy of Sciences of the United States of America* 104.39, pp. 15248–15253. ISSN: 00278424. DOI: 10.1073/pnas.0702872104.

Schmucki, Edgar et al. (2014). "Evaluation of modelled snow depth and snow water equivalent at three contrasting sites in Switzerland using SNOWPACK simulations driven by different meteorological data input". In: *Cold Regions Science and Technology* 99, pp. 27–37. ISSN: 0165232X. DOI: 10.1016/j.coldregions.2013.12.004. URL: http://dx.doi.org/10.1016/j.coldregions.2013.12.004.

Schneebeli, M. (1995). "Development and stability of preferential flow paths in a layered snowpack". In: *Biogeochemistry of seasonally snow-covered catchments. Proc. symposium, Boulder, 1995* December, pp. 89–95.

Singh, Pratap et al. (1998). "The role of snowpack in producing floods under heavy rainfall". In: *IAHS-AISH Publication* 248.248, pp. 89–95. ISSN: 01447815.

Stearns, Charles R. & George A. Weidner (2011). *Sensible and latent heat flux estimates in Antarctica*, pp. 109–138. DOI: 10.1029/ar061p0109.

Sui, Jueyi & Gero Koehler (2001). "Rain-on-snow induced flood events in southern Germany". In: *Journal of Hydrology* 252.1-4, pp. 205–220. ISSN: 00221694. DOI: 10.1016/S0022-1694(01)00460-7.

Swain, Daniel L. et al. (2018). "Increasing precipitation volatility in twenty-first-century California". In: *Nature Climate Change* 8.5, pp. 427–433. ISSN: 17586798. DOI: 10.1038/s41558-018-0140-y. URL: http://dx.doi.org/10.1038/s41558-018-0140-y.

Techel, F. & C. Pielmeier (2011). "Point observations of liquid water content in wet snow – Investigating methodical, spatial and temporal aspects". In: *Cryosphere* 5.2, pp. 405–418. ISSN: 19940416. DOI: 10.5194/tc-5-405-2011.

Trenberth, Kevin E. (2011). "Changes in precipitation with climate change". In: *Climate Research* 47.1-2, pp. 123–138. ISSN: 0936577X. DOI: 10.3354/cr00953.

Trubilowicz, Joel W. & R. Dan Moore (2017). "Quantifying the role of the snowpack in generating water available for run-off during rain-on-snow events from snow pillow records". In: *Hydrological Processes* 31.23, pp. 4136–4150. ISSN: 10991085. DOI: 10.1002/hyp.11310.

USGS (1997). *Flood of January 1997 in the Truckee River Basin, Western Nevada*. Tech. rep. August, pp. 1–2.

Waldner, Peter A. et al. (2004). "Effect of snow structure on water flow and solute transport". In: *Hydrological Processes* 18.7, pp. 1271–1290. ISSN: 08856087. DOI: 10.1002/hyp.1401.

Watts, Tom et al. (2016). "Brief communication: Improved measurement of ice layer density in seasonal snowpacks". In: *Cryosphere* 10.5, pp. 2069–2074. ISSN: 19940424. DOI: 10.5194/tc-10-2069-2016.

Wever, N., C. Fierz, et al. (2014). “Solving Richards Equation for snow improves snowpack meltwater runoff estimations in detailed multi-layer snowpack model”. In: *Cryosphere* 8.1, pp. 257–274. ISSN: 19940416. DOI: 10.5194/tc-8-257-2014.

Wever, N., T. Jonas, et al. (2014). “Model simulations of the modulating effect of the snow cover in a rain-on-snow event”. In: *Hydrology and Earth System Sciences* 18.11, pp. 4657–4669. ISSN: 16077938. DOI: 10.5194/hess-18-4657-2014.

Wever, N., Sebastian Würzer, et al. (2016). “Simulating ice layer formation under the presence of preferential flow in layered snowpacks”. In: *Cryosphere* 10.6, pp. 2731–2744. ISSN: 19940424. DOI: 10.5194/tc-10-2731-2016.

White, Allen B. et al. (2019). “Winter storm conditions leading to excessive runoff above California’s Oroville dam during January and February 2017”. In: *Bulletin of the American Meteorological Society* 100.1, pp. 55–69. ISSN: 00030007. DOI: 10.1175/BAMS-D-18-0091.1.

Würzer, Sebastian et al. (2016). “Influence of Initial Snowpack Properties on Runoff Formation during Rain-on-Snow Events”. In: *Journal of Hydrometeorology* 17.6, pp. 1801–1815. ISSN: 1525-755X. DOI: 10.1175/jhm-d-15-0181.1.

Yamaguchi, Satoru, Atsushi Sato, & Michael Lehning (2004). “Application of the numerical snowpack model (SNOWPACK) to the wet-snow region in Japan”. In: *Annals of Glaciology* 38, pp. 266–272. ISSN: 02603055. DOI: 10.3189/172756404781815239.

Zwart, Costijn (2007). “Significance of new snow properties for snow-cover development”. In: 9.March 2006, p. 2. URL: http://www.academia.edu/18041227/Significance_of_new_snow_properties_for_snow-cover_development.